DOI: 10.1002/cssc.201000338

Polyaniline-Based Conducting Polymer Compositions with a High Work Function for Hole-Injection Layers in Organic Light-Emitting Diodes: Formation of Ohmic Contacts

Mi-Ri Choi,[a] Seong-Hoon Woo,[a] Tae-Hee Han,[a] Kyung-Geun Lim,[a] Sung-Yong Min,[a] Won Min Yun,[b] Oh Kwan Kwon,[b] Chan Eon Park,[b] Kwan-Do Kim,[c] Hoon-Kyu Shin,[c] Myeong-Suk Kim,[d] Taeyong Noh,[d] Jong Hyeok Park,[e] Kyoung-Hwan Shin,[f] Jyongsik Jang,[f] and Tae-Woo Lee*[a]

It is a great challenge to develop solution-processed, polymeric hole-injection layers (HILs) that perform better than small molecular layers for realizing high-performance small-molecule organic light-emitting diodes (SM-OLEDs). We have greatly improved the injection efficiency and the current efficiency of SM-OLEDs by introducing conducting polymer compositions composed of polyaniline doped with polystyrene sulfonate and perfluorinated ionomer (PFI) as the HIL. During single spin-coating of conducting polymer compositions, the PFI layer was self-organized at the surface and greatly increased the film work function. It enhanced hole-injection efficiency and current efficiency by introducing a nearly ohmic contact and improving electron blocking. Our results demonstrate that solution-processed polyaniline HILs with tunable work functions are good candidates for reducing process costs and improving OLED performance.

Introduction

Organic light-emitting diodes (OLEDs) have attracted much attention because they are desirable candidates for solid-state lighting devices as well as large-area, high-resolution, fast-response, full-color flexible displays.[1,2] Beyond the other allures offered by OLEDs, the technology is more environmentally sustainable than that of conventional liquid-crystal displays. Achieving high efficiency in OLED devices is one of the most crucial issues for commercialization. Tremendous efforts have been made to overcome the high hole-injection barrier between the anode and the emitting layer. Optically transparent indium tin oxide (ITO) has been generally used as the anode for organic optoelectronic devices. Because ITO possesses a relatively low work function (WF = 4.9 eV), new hole-injection layers (HILs) with a high ionization potential (IP) are required for efficient hole injection. Small molecules, such as copper phthalocyanine (CuPc, IP = 5.0 eV); 4,4′,4″-tris(3-methylphenyl-*N*-phenylamino)triphenylamine (m-MTDATA, IP = 5.1 eV); and 4,4′,4″-tris[*N*-(2-naphthyl)-*N*-phenylamino]triphenylamine (2TNATA, IP = 5.1 eV), have been preferentially employed as HILs in vacuum-deposited, small-molecule organic light-emitting diodes (SM-OLEDs). Although conducting polymers such as poly(ethylene dioxythiophene) doped with polystyrene sulfonate (PEDOT:PSS, WF = 5.0–5.2 eV) and polyaniline doped with PSS (PANI:PSS, WF = 5.2–5.3 eV) are alternatives to small-molecule HILs in SM-OLEDs, only a few reports have described solution-processed HILs in SM-OLEDs because of the remaining high injection barrier and low efficiency.[3,4] Recently, high-performance, solution-processable HILs have attracted much attention in OLED research for the development of highly efficient and stable SM-OLED panels fabricated by a solution process.[5]

Current research requires new strategies for developing solution processable and efficient hole-injection buffer layers for high-performance SM-OLEDs. Both increased hydrophobicity and high WF values of the films are necessary for stable and

[a] *M.-R. Choi,[+] S.-H. Woo,[+] T.-H. Han, K.-G. Lim, S.-Y. Min, Prof. T.-W. Lee*
Department of Materials Science and Engineering
Pohang University of Science and Technology (POSTECH)
San 31 Hyoja-dong, Nam-gu, Pohang, Gyeongbuk 790-784 (Korea)
Fax: (+82) 54-279-2399
E-mail: twlee@postech.ac.kr

[b] *W. M. Yun, Dr. O. K. Kwon, Prof. C. E. Park*
Department of Chemical Engineering
Pohang University of Science and Technology (POSTECH)
San 31 Hyoja-dong, Nam-gu, Pohang, Gyeongbuk 790-784 (Korea)

[c] *K.-D. Kim, Dr. H.-K. Shin*
National Center for Nanomaterials Technology
San 31 Hyoja-dong, Nam-gu, Pohang, Gyungbuk 790-784 (Korea)

[d] *Dr. M.-S. Kim, Dr. T. Noh*
Samsung Mobile Displays
Mt. 14-1, Nongseo-dong, Giheung-gu, Yongin-si
Gyeonggi-do 446-712 (Korea)

[e] *Prof. J. H. Park*
Department of Chemical Engineering
Sungkyunkwan University
Suwon, Gyeonggi-do 440-746 (Korea)

[f] *K.-H. Shin, J. Jang*
School of Chemical and Biological Engineering
Seoul National University
Seoul 151-742 (Korea)

[+] *These authors contributed equally to this work.*

efficient hole injection in the devices. From this viewpoint, the introduction of a perfluorinated ionomer (PFI) into the conducting polymer compositions could increase the hydrophobicity and WF.[6–8] From a practical point of view, a great challenge is to develop solution-processable HILs that perform better than small-molecule HILs in vacuum-deposited, multilayered SM-OLEDs. In this manner, the production cost and processing time of state-of-the-art SM-OLEDs for commercial production can also be reduced by removing the HIL vacuum-deposition process.

Herein, we introduce solution-processable polyaniline compositions composed of PANI:PSS and PFI (PANI:PSS/PFI) with high WF values. To the best of our knowledge, this work is the first report regarding water-dispersed polyaniline-based conducting polymers with tunable WF values. We employed the polyaniline compositions as HILs to achieve enhanced current efficiencies in SM-OLEDs. We compared the characteristics of OLED devices using the PANI:PSS/PFI layers with those of devices that employ a conventional small-molecule HIL, 2TNATA. We characterized the surface of the spin-cast films by X-ray photoelectron spectroscopy (XPS) and ultraviolet photoelectron spectroscopy (UPS). The results confirmed that high concentrations of PFI in the composition caused high concentrations of PFI at the film surface, thereby increasing the WF. We analyzed the hole-injection efficiencies of the hole-only device formed from the PANI:PSS/PFI composition and investigated the relationship between WF, injection efficiency, and current efficiency. We demonstrated that the newly formulated solution-processable HIL notably enhanced the current efficiency compared with a small-molecule HIL in vacuum-deposited SM-OLEDs due to the formation of nearly ohmic hole-injection contacts.

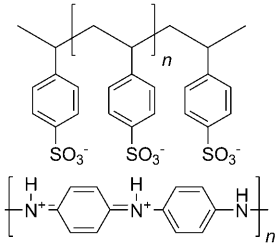

PANI:PSS

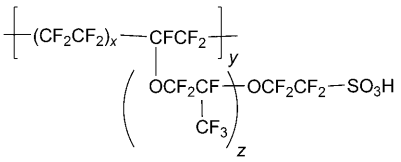

PFI

Results and Discussion

Surface analysis of the compositions

Water-dispersible PANI:PSS at a 1:6 weight ratio was prepared by oxidative polymerization of aniline in the presence of excess hydrochloric acid by adjusting the feed ratio of the aniline monomer, PSS, and hydrochloric acid as a protonating agent/dopant. The PANI:PSS nanoparticles did not precipitate due to the strong electrostatic interactions between PANI and PSS, and they were well dispersed in an aqueous solution.[9] We newly formulated conducting polymer compositions in a solvent mixture of water and alcohol. We systematically changed the ratio of PFI to PANI:PSS in the conducting polymer compositions that were employed as HILs in OLEDs. Before measuring the OLED device performance, we analyzed the surface of films that were spin-cast in conducting polymer compositions (PANI:PSS/PFI, abbreviated as PNPF). The WF value as a function of the composition was measured by UPS. The results are summarized in Table 1; these results show that

Table 1. The work function values of the polyaniline-based conducting polymer compositions used for the hole-injection layers.

Sample code	PANI	PSS	PFI	WF [eV]
PANI:PSS	1	6	–	5.19
PNPF161	1	6	1.68	5.88
PNPF81	1	6	3.37	5.80
PNPF41	1	6	6.73	5.83
PNPF21	1	6	13.48	5.98

the WF value increased significantly upon addition of PFI. We obtained a very high WF value for PNPF21 (5.98 eV) relative to that of a conventional conducting polymer, PEDOT:PSS (5.18 eV), or the ionization potential of a conventional small molecule, 2TNATA (5.1 eV). Perfluorinated ionic polymers significantly increased the surface ionization potential when they were preferentially located at a film surface, as predicted by DFT calculations.[6] Therefore, as the PFI concentration increased in the conducting polymer film, the WF value increased. It should be noted that the addition of small amounts of PFI to the PANI:PSS (1:6) composition in a weight ratio of 1:6:1.6 (PNPF161 in Table 1) yielded a very high film WF value (5.88 eV). In contrast, the film prepared from the PEDOT:PSS/PFI composition with the same ratio (1:6:1.6 by weight, i.e., AlPF161 in Reference [7]) had a much lower WF value of 5.55 eV.[6] The PEDOT:PSS/PFI composition with a ratio of 1:2.5:2.92 also yielded a much lower WF value of 5.26 eV.[8] This systematic study indicated that the PFI surface enrichment in the case of using the PANI:PSS/PFI compositions was larger than that achieved by using the PEDOT:PSS/PFI compositions.

We used XPS to investigate the molecular distribution at the surface of the HILs. Figure 1 shows the C 1s core level spectra of the films spin-cast from PANI:PSS and PANI:PSS/PFI (PNPF41). Gaussian–Lorentzian fitting permitted deconvolution of the C 1s spectrum into four peaks, at 284.8 (C–C/C–H), 285.9 (C=N), 286.7 (C–O), and 288.1 eV (C=O). The highest binding energy peak at 288.1 eV corresponded to the carbonyl carbon atoms (C=O) formed by the attack of water molecules during the electrochemical reaction.[10] The C 1s spectrum of the film composed of PANI:PSS and PFI contained two additional peaks (Figure 1b). These two peaks were attributed to the presence of PFI. The strong peak at 291.6 eV was assigned to the superposition of signals from CF_2, CF–O, and CF_2–O groups in the polymer chains.[11] The highest binding energy at 293.9 eV was assigned to CF_3 and the total CF_x ($x = 1$–3) contribution. The lower binding energy

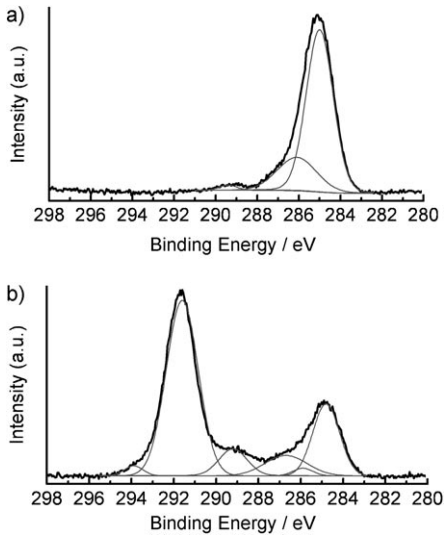

Figure 1. The C 1s core level spectra of a) PANI:PSS and b) PANI:PSS/PFI (PNPF41) films measured by XPS.

contributions at 289.2, 286.7, and 284.8 eV arose from contamination by PFI and PANI:PSS.[11]

The ratio of PFI to PSS at the surface was estimated from the F 1s and S 2p spectra on the film surfaces. The area beneath the F 1s spectrum indicated the quantity of PFI present, and the S 2p spectrum indicated the quantity of sulfonic acid in the PFI and PSS. The atomic composition percentage, calculated from the XPS peaks,[11] determined the ratio of PFI to PSS at the surface. As summarized in Table 2, the F 1s peak area arising from PFI was much larger than the S 2p peak area formed due to PANI:PSS because PFI was preferentially positioned at the surface through self-organization during spin-coating of the PANI:PSS/PFI composition. To compare the relative composition of F and S atoms at the surface from two different core level spectra of F 1s and S 2p, we used an empirically derived set of atomic sensitivity factor of S 2p relative to F 1s obtained from a combination of data from Varian IEE and Physical Electronics (Perkin–Elmer) 550 spectrometers.[12]

Table 2. The ratio of the area under the F 1s core level spectra to the area under the S 2p core level spectra of various polymeric hole-injection layers measured by XPS.

Sample code	Surface area S 2p	Surface area F 1s	Atomic ratio F/S_{total}[a]	Atomic ratio $F/S_{PANI:PSS}$[b]
PANI:PSS	40.9	–	–	–
PNPF161	56.3	5496.2	97.6	282.2
PNPF81	55.9	4415.0	78.9	167.6
PNPF41	63.3	5507.6	87.0	208.4
PNPF21	136.1	15441.5	113.5	473.0

[a] The area under the F spectrum is only attributed to the PFI, but the area under the S spectrum is attributed to PANI:PSS and PFI. F/S_{total} is the ratio of F from PFI to S from both PANI:PSS and PFI. [b] To investigate the ratio of PFI to PANI:PSS at the film surface, we calculated the $F/S_{PANI:PSS}$ ratio, which is the ratio of F from PFI to S from PANI:PSS.

Table 2 shows that even a small addition of PFI to PANI:PSS in the PNPF161 composition greatly increased the richness of PFI at the surface relative to the other components, which was consistent with the very high WF value (5.88 eV), as shown in Table 1. This confirmed that PFI underwent very good self-organization toward the film surface when it was incorporated into the PANI:PSS composition. The surface information depth was estimated by using $3\lambda\sin\theta$ to be 57 Å, in which the inelastic mean free path, λ, of the S 2p electrons was 27 Å and the take-off angle θ was 45°. Therefore, the surface composition of the films obtained from XPS measurements reflected the surface information to a depth of nearly 6 nm. The ratio of the F 1s peak area from the PFI to the S 2p peak area from the PANI:PSS at the surface was high, as shown in Table 2. This implies that PFI self-organizes preferentially at the film surface, owing to the low surface energy and low compatibility with hydrocarbon polymer chains. As a result, the surface was mainly found to be covered with the PFI component, independent of the formulation PFI concentration. Overall, the atomic ratio at the surface tended to increase as the PFI concentration increased in all compositions (PANI:PSS/PFI) except for PNPF161. The high PFI surface concentration increased the WF values (Tables 1 and 2) because the perfluorinated chains provided an ionization potential that was higher than that of the hydrocarbon chains.[6]

The work function of the PANI:PSS (5.19 eV) layer was slightly higher than or similar to that of the PEDOT:PSS (5.18 eV) layer. Previously, Jang et al. reported that PANI:PSS films prepared by an identical synthetic route yielded a high WF value (5.27 eV) attributed to a ratio of PSS to PANI (10:1 w/w) that was higher than the standard PSS to PEDOT ratio (6:1 w/w) in the commercial product for the HIL (Baytron P VP AI4083).[12] A systematic study of the surface WF as a function of the ratio of PSS to PEDOT at the film surface was recently described by our group.[13] The WF value could be systematically tuned by controlling the PSS to PEDOT ratio at the film surface. This can also apply to the PANI:PSS complex system. The observation of a WF value for the PANI:PSS (1:6 w/w) system that was lower than that observed previously for PANI:PSS (1:10 w/w) systems can be understood similarly by the surface characteristics of the PEDOT:PSS system.[13]

Injection efficiency of hole-only devices

We fabricated hole-only devices composed of ITO/HIL (50 nm)/*N*,*N*′-*bis*(naphthalen-1-yl)-*N*,*N*′-*bis*(phenyl) benzidine (NPB; 200 nm)/Al with various HILs (Figure 2a). When PFI was added to the PANI:PSS composition, the hole current improved significantly, as shown in Figure 3. This demonstrated the good hole-injection capabilities of the PNPF series of HILs. We compared the threshold voltages (V_{th}), defined as the voltage at which the current density increased sharply in the low-voltage regime using a log–log plot. Figure 3b shows that V_{th} was 1.65 V for the PANI:PSS device, but V_{th} was reduced (0.85–0.98 V) in the devices using the PNPF series of HILs. The V_{th} tended to decrease slightly as the PFI concentration increased (0.98 V for PNPF161, 0.92 V for PNPF81, 0.86 V for PNPF41, and

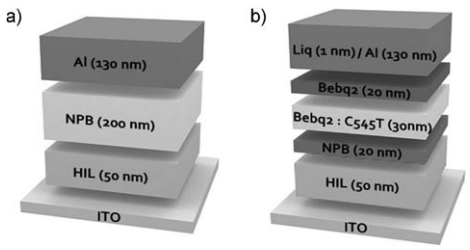

Figure 2. Device structures using PANI:PSS/PFI as the hole-injection layer. a) Hole-only device structure and b) device structure of the SM-OLEDs. $Bebq_2$ = *bis*(10-hydroxybenzo[h]quinolinato)beryllium, C545T = 10-(2-benzothiazolyl)-1,1,7,7-tetramethyl-2,3,6,7-tetrahydro-1H,5H,11H-[1]benzopyrano-[6,7,8-ij]quinolizin-11-one, Liq = 8-hydroxyquinoline lithium.

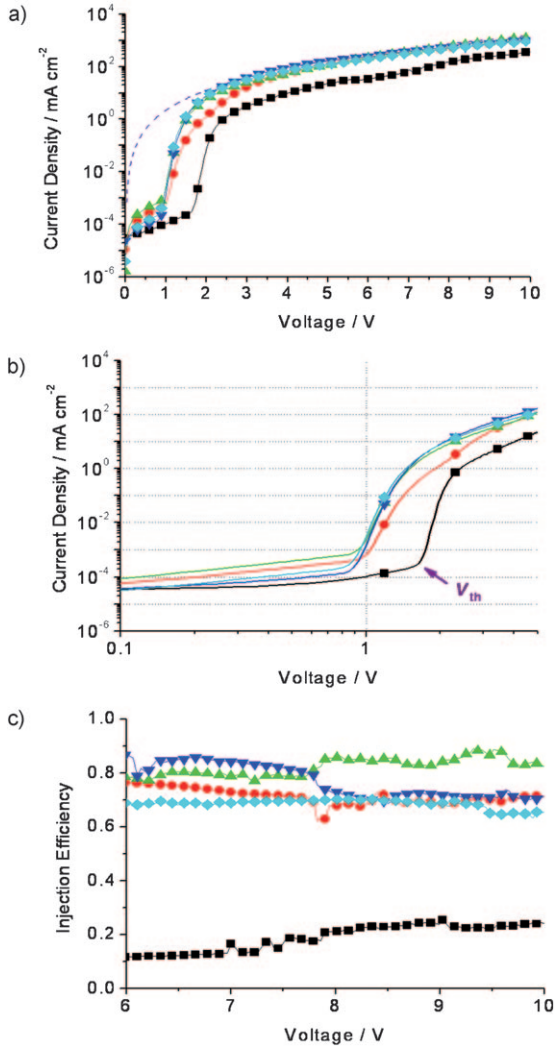

Figure 3. The current density versus voltage characteristics (a, b) and injection efficiencies (c) of hole-only devices with the structure ITO/HIL (50 nm)/NPB (200 nm)/Al, in which the HILs were the PNPF series or PANI:PSS. ■: PANI:PSS, ●: PNPF161, ▲: PNPF81, ▼: PNPF41, ◆: PNPF21, and -----: calculated current density. a) Semi-log plot, b) log–log plot, and c) injection efficiency.

0.85 V for PNPF21). The devices with the PNPF series of HILs showed similar hole current densities, which indicated that the high WF values of the HILs were mainly pinned to the NPB HOMO level (−5.4 eV).[14] We observed a lower current density of PNPF161 below 4 V despite a high WF value. A small addition of PFI to PANI:PSS caused extensive self-organization of PFI at the film surface, but could not result in a gradient increase of WF throughout the film due to the low PFI content. Therefore, the lower current density of the PNPF161 HIL device at low voltages despite the high surface WF demonstrated the importance of a gradient film morphology throughout the HIL layer for good hole injection.[6] In the hole-only PNPF series of HIL devices, the current density versus voltage characteristics at low voltages below the current density threshold voltages clearly followed Ohm's law ($J \propto V$), indicative of a good hole-injection contact.

The current densities of hole-only devices featuring ohmic contacts can be calculated according to the space-charge-limited current (SCLC) model. By combining the SCLC and the Poole–Frenkel equation,[15] the field-dependent SCLC can be described by Equation (1):

$$J = \frac{9}{8}\varepsilon\varepsilon_0\frac{E^2}{L}\mu_0\exp(\beta\sqrt{E}) \quad (1)$$

in which ε is the relative dielectric constant, ε_0 is the permittivity of free space, E is the electric field, L is the thickness of the organic layer, μ_0 is the zero-field mobility, and β is the Poole–Frenkel factor. Using Equation (1), we calculated the current densities of hole-only devices with the structure ITO/HIL/NPB (200 nm)/Al as a function of bias voltage by using the values for μ_0 and β ($\mu_0 = 3\times10^{-5}$ and $\beta = 0.004$) reported in the literature.[15] The calculated current density versus voltage curves are plotted together with the measured current densities of the hole-only devices in Figure 3a. The calculated SCLC current densities were almost identical to the measured PNPF-series HIL device current densities. This implies that the hole-only NPB devices that use the PNPF series of HILs are bulk-limited. We assessed the injection efficiency for various HILs according to Equation (2):[16]

$$\eta = \frac{J_{INJ}}{J_{BULK}} \quad (2)$$

in which J_{INJ} is the current density supplied by the contact and J_{BULK} represents the maximum current density carried by the organic layer, assuming ideal ohmic contact, which corresponds to the calculated current density of the hole-only device. The hole-injection efficiencies from each HIL layer (PANI:PSS and the PNPF series) to the NPB layer were determined as a function of voltage, as shown in Figure 3c. The injection efficiencies of the PNPF series of HILs ranged from 0.7 to 0.9 (i.e., close to 1), whereas the injection efficiency from the PANI:PSS HIL layer was less than 0.2. This implies that the PNPF series of HILs produced nearly ohmic hole-injection contacts, whereas the PANI:PSS HIL did not. In other words, the PNPF series of HILs produced devices that followed the bulk-limited conduction mechanism, whereas PANI:PSS produced devices that followed the injection-limited conduction mechanism. The injection efficiencies did not show a meaningful dependence

on the PFI concentration in the PNPF series of compositions. This was ascribed to the fact that PFI was preferentially positioned at the surface through self-organization during a single spin-coating of the composition composed of PANI:PSS and PFI.[6] The surface-enriched PFI layer greatly increased the WF value and, therefore, greatly facilitated hole injection by producing nearly ohmic contacts.

SM-OLEDs using the PNPF series as HILs

We fabricated SM-OLEDs using the newly formulated conducting polymer compositions (PANI:PSS/PFI) as the HILs, and we compared the *I–V–L* characteristics with those of a conventional small-molecule HIL (2TNATA, the device structure is shown in Figure 2b). The *I–V–L* characteristics of the fluorescent green light-emitting diodes employing each HIL are plotted in Figure 4. Figure 4a shows the current density versus voltage characteristics for devices with each HIL. The current densities of the devices employing polymeric HILs were higher by an order of magnitude than that of the device that used a small-molecule HIL. The current densities of devices using the polymeric HILs were similar. The luminance versus voltage characteristics shown in Figure 4b followed the same trend as the current density versus voltage characteristics. When the HILs containing a higher concentration of the PFI were employed, the luminance was enhanced. As a result, the current density and luminance values for the devices increased as the concentration of PFI increased, which was attributed to the increased WF value and thus facilitated hole injection.

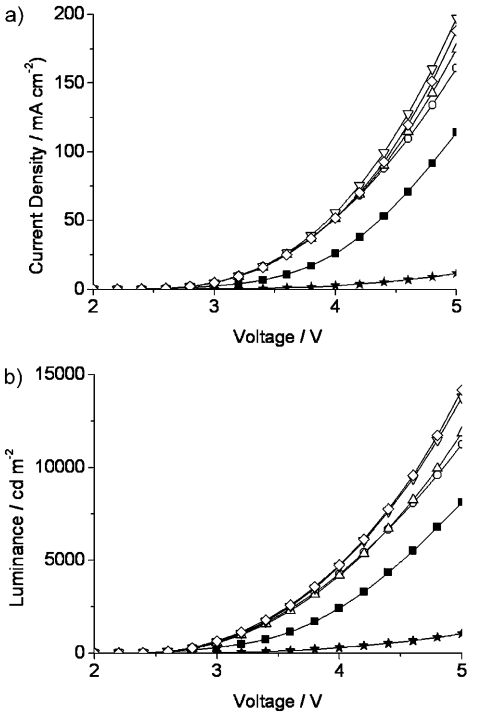

Figure 4. (a) Current density versus voltage, and (b) luminance versus voltage characteristics of OLEDs, recorded using different HILs. ■: PANI:PSS, ○: PNPF161, △: PNPF81, ▽: PNPF41, ◇: PNPF21, and ★: 2TNATA. The device structure measured was ITO/HIL/NPB/Bebq$_2$+C545T (2%)/Bebq$_2$/Liq/Al.

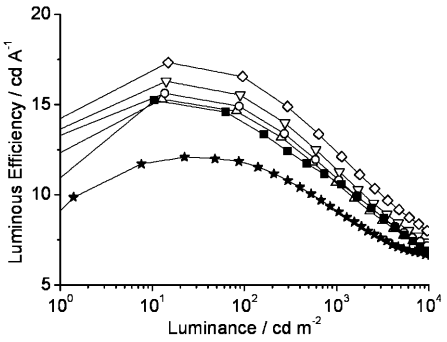

Figure 5. The current efficiencies of the OLEDs using PANI:PSS/PFI-series and PANI:PSS HILs in the structure ITO/HIL/NPB/Bebq$_2$ + C545T (2%)/Bebq$_2$/Liq/Al. ■: PANI:PSS, ○: PNPF161, △: PNPF81, ▽: PNPF41, ◇: PNPF21, and ★: 2TNATA.

We compared the current efficiencies of devices fabricated using a polymeric HIL and devices fabricated using 2TNATA. The 2TNATA device showed a current efficiency of 12.1 cd A^{-1}. When the PANI:PSS conducting polymer was employed as the HIL, a higher efficiency of 15.2 cd A^{-1} was obtained. The maximum current efficiency (17.3 cd A^{-1}) was achieved in the polymeric HIL device that contained the highest concentration of PFI (PNPF21). Figure 3 shows that the hole-injection capabilities of the PNPF series of HILs in the hole-only devices does not depend heavily on the relative composition. However, the device current efficiencies depended on the PFI concentration in the PNPF series of HIL devices (Figure 5), suggesting that another mechanism was available for improving the current efficiency.

In our device structure, the overlying layer of our HIL is the NPB layer with an ionization potential of 5.4 eV.[14] If the WF value of our HIL is higher than that of NPB, the high WF of the HIL does not dominantly affect hole-injection capability, which results in similar hole-injection efficiency for our PNPF series of HILs. In this case, the electron-blocking ability of surface-enriched PFI layer is the main factor for improving current efficiency of the devices using PANI:PSS/PFI HILs. The thicker surface-enriched PFI layers blocked electrons coming from the emitting layer to be accumulated close to the HIL interface in the devices. As the accumulated electrons gathered at the interface, they were partly transferred back to the NPB/emitting layer (EML) interface to engage in radiative electron–hole recombination. Therefore, the PFI-enriched surface layer compensated for the poor electron-blocking properties of the NPB layer. As a result, efficient hole injection and electron blocking by the PNPF series of HILs improved the electron–hole recombination rate in devices, which resulted in a high current efficiency.

These results clearly demonstrate that improved device performances were achieved by using solution-processed PANI:PSS/PFI HILs in place of PANI:PSS and small-molecule HILs (2TNATA) in SM-OLEDs.

Conclusion

This work demonstrated the preparation of high-efficiency SM-OLEDs by employing polyaniline-based conducting polymer compositions containing PFI as the HIL through a single spin-coating self-organization process. The PFI was preferentially positioned at the surface of the hole-injection layer and increased the WF value, as measured by UPS and XPS. The PANI:PSS/PFI layers showed much higher WF values (5.8–6.0 eV) than the conventional PEDOT/PSS (5.0–5.2 eV) and 2TNATA (5.1 eV) layers. The higher WF values produced by PFI lowered the hole-injection barrier from the HIL to the EML. However, the WF values of the HILs tended to be pinned to the HOMO level of the hole transporting layer (NPB) so that the hole-injection efficiencies were comparable (0.7–0.9) and independent of the PFI concentration in the PANI:PSS/PFI composition. The high hole-injection efficiencies close to one imply that the PANI:PSS/PFI HILs produced a nearly ohmic hole-injection contact. We achieved a current efficiency of 17.3 cd A^{-1} using our HIL, which was much higher than that obtained by using small-molecule HILs (12.1 cd A^{-1}). The improved efficiency was attributed to improved hole-injection and electron-blocking properties at the PFI-enriched surface. This work clearly demonstrates the utility of polymeric HILs with high WF values and self-organized chain morphologies for the fabrication of vacuum-deposited SM-OLEDs. Since the polymeric HILs outperformed a small-molecule HIL (2TNATA) in terms of current efficiency, the use of these new polymeric HILs in OLEDs can improve the performance of conventional SM-OLED devices as well as simplify the vacuum fabrication process by the introduction of a nonvacuum solution process to reduce fabrication costs.

Experimental Section

Synthesis of the PANI:PSS solution: Water-dispersible PANI:PSS synthesized at a 1:6 weight ratio was used. The aqueous PSS solution was produced by adding a quantity of PSS to water followed by stirring. The PANI:PSS solution was synthesized by oxidative polymerization of aniline in the presence of HCl and PSS. Aniline monomers (0.53 mmol) were introduced dropwise to a 0.5 M aqueous solution of HCl (35 mL) followed by stirring for 2 h. Then, as-prepared aqueous PSS solution (0.6 g) was added to the mixed solution followed by stirring for 1 h. The polymerization of aniline proceeded in the presence of ammonium persulfate (APS; 0.69 mmol) as the oxidizing agent over 12 h at 25 °C. After polymerization, a dark-green solution of PANI:PSS was obtained.

Device fabrication: The hole-injection layers (PANI:PSS, PANI:PSS/PFI) about 50 nm thick were spin-coated on top of a precleaned ITO/glass substrate. PANI:PSS and PANI:PSS/PFI compositions were baked sequentially on a hot plate in air at 150 °C for 10 min then in a N_2 glove box at 150 °C for 10 min. Organic layers consisting of 20 nm thick NPB, 30 nm thick $Bebq_2$:C545T, and 20 nm thick $Bebq_2$ were sequentially deposited on the hole-injection layers under high vacuum ($< 5\times10^{-7}$ torr). Cathode layers of Liq (1 nm)/Al (130 nm) were deposited under high vacuum ($< 5\times10^{-7}$ torr). The devices were encapsulated with a glass lid by using a UV-curable epoxy resin.

Device characterization: The *I–V–L* characteristics were obtained by using a Keithley 236 source measurement unit and a Minolta CS2000 Spectroradiometer. The device lifetimes were recorded by using a McScience Polaronix OLED Lifetime Test System.

Acknowledgements

This research was supported by the Basic Research Program through the National Research Foundation of Korea (NRF), funded by the Ministry of Education, Science and Technology (nos. 2009-0067533, 2009-0075025, and 2009-0090177). This work was also supported by a National Research Foundation of Korea Grant funded by the Korean Government (MEST) (NRF-2009-C1AAA001-0093524). This work was also supported by Undergraduate Research Program through the Korea Foundation for the Advancement of Science & Creativity (2009-1-45)

Keywords: charge-carrier injections · conducting materials · organic light-emitting diodes · materials science · polymers

[1] a) C. W. Tang, S. A. VanSlyke, *Appl. Phys. Lett.* **1987**, *51*, 913–915; b) P. L. Burn, S.-C. Lo, I. D. W. Samuel, *Adv. Mater.* **2007**, *19*, 1675–1688; c) P. K. H. Ho, J.-S. Kim, J. H. Burroughes, H. Becker, S. F. Y. Li, T. M. Brown, F. Cacialli, R. H. Friend, *Nature* **2000**, *404*, 481–484; d) A. J. Sandee, C. K. Williams, N. R. Evans, J. E. Davies, C. E. Boothby, A. Kohler, R. H. Friend, A. B. Holmes, *J. Am. Chem. Soc.* **2004**, *126*, 7041–7048; e) K. H. Yim, Z. Zheng, Z. Liang, R. H. Friend, W. T. S. Huck, J. S. Kim, *Adv. Funct. Mater.* **2008**, *18*, 1012–1019; f) M. H. Song, D. Kabra, B. Wenger, R. H. Friend, H. J. Snaith, *Adv. Funct. Mater.* **2009**, *19*, 2130–2136.

[2] a) S. Reineke, F. Lindner, G. Schwartz, N. Seidler, K. Walzer, B. Lüssem, K. Leo, *Nature* **2009**, *459*, 234–238; b) T.-W. Lee, T. Noh, B.-K. Choi, M.-S. Kim, D. W. Shin, J. Kido, *Appl. Phys. Lett.* **2008**, *92*, 043301; c) B. W. D'Andrade, S. R. Forrest, *Adv. Mater.* **2004**, *16*, 1585–1595; d) T.-W. Lee, J. Hwang, S.-Y. Min, *ChemSusChem* **2010**, *3*, 1021–1023.

[3] A. Elschner, F. Bruder, H. W. Heuer, F. Jonas, A. Karbach, S. Kirchmeyer, S. Thurm, R. Wehrmann, *Synth. Met.* **2000**, *111*, 139–143.

[4] T. Y. Kim, M. Suh, S. J. Kwon, T. H. Lee, J. E. Kim, Y. J. Lee, J. H. Kim, M. P. Hong, K. S. Suh, *Macromol. Rapid Commun.* **2009**, *30*, 1477–1482.

[5] a) C.-H. Hsu, Y. Shen, E. M. Smith, D. D. LeCloux, H. Skulason, S. Kim, I. D. Parker, *SID Symposium Digest* **2006**, *37*, 49; b) W. F. Feehery , *SID Symposium Digest* **2007**, *38*, 1834–1836; c) M. O'Regan, *SID Symposium Digest* **2009**, *40*, 600–602.

[6] T.-W. Lee, Y. Chung, O. Kwon, J.-J. Park, *Adv. Funct. Mater.* **2007**, *17*, 390–396.

[7] K. R. Choudhury, J. Lee, N. Chopra, A. Gupta, X. Jiang, F. Amy, F. So, *Adv. Funct. Mater.* **2009**, *19*, 491–496.

[8] T.-W. Lee, O. Kwon, M.-G. Kim, S. H. Park, J. Chung, S. Y. Kim, Y. Chung, J.-Y. Park, E. Han, D. H. Huh, J.-J. Park, L. Pu, *Appl. Phys. Lett.* **2005**, *87*, 231106.

[9] J. Jang, J. Ha, J. Cho, *Adv. Mater.* **2007**, *19*, 1772–1775.

[10] L.-M. Huang, W.-R. Tang, T.-C. Wen, *J. Power Sources* **2007**, *164*, 519–526.

[11] D. Susac, M. Kono, K. C. Wong, K. A. R. Mitchell, *Appl. Surf. Sci.* **2001**, *174*, 43–50.

[12] J. Jang, J. Ha, K. Kim, *Thin Solid Films* **2008**, *516*, 3152–3156.

[13] T.-W. Lee, Y. Chung, *Adv. Funct. Mater.* **2008**, *18*, 2246–2252.

[14] Q. L. Huang, J. F. Li, G. A. Evmenenko, P. Dutta, T. J. Marks, *Chem. Mater.* **2006**, *18*, 2431–2442.

[15] T. Y. Chu, O. K. Song, *Appl. Phys. Lett.* **2007**, *90*, 203512.

[16] B. Jiao, Z. Wu, X. Yan, X. Hou, *Appl. Phys. A* **2010**, *98*, 239–243.

Received: October 6, 2010
Published online on January 24, 2011

